$$Z_{a1} = Z_{a3} = \sqrt{z_{11}/y_{11}} \tag{19a}$$

$$Z_{b1} = Z_{b2} = Z_{b3} = \sqrt{(z_{11} + \sqrt{2}\,z_{12})/(y_{11} + \sqrt{2}\,y_{12})} \tag{19b}$$

$$Z_{c1} = Z_{c2} = Z_{c3} = \sqrt{(z_{11} - \sqrt{2}\,z_{12})/(y_{11} - \sqrt{2}\,y_{12})}. \tag{19c}$$

The experimental results given in [2] agree well with the theoretical predictions since the conditions given above are approximately satisfied for the experimental structure which consists of identical relatively loosely coupled microstrip lines. However, for the general case of three-line microstrip structures the analytical results given in this paper can be utilized to formulate design procedures for couplers and other circuit elements.

III. Conclusions

Symmetrical three-line microstrip or other inhomogeneous structures may be studied in terms of the normal uncoupled wave modes and six-port circuit parameters of the system. The expressions for the propagation constants, characteristic impedances, and six-port parameters have been derived explicitly in terms of the distributed self- and mutual- impedances and admittances per unit length of the lines. For the case of coupled microstrip lines, the results obtained should be useful in the study and design of couplers and other circuit elements. The theory applies to any symmetrical coupled three-line dispersive, lossy, passive, or reciprocal-active system and may be used to study such systems in terms of their equivalent self- and mutual-line parameters.

References

[1] V. Rizzoli and A. Lipparini, "Accurate analysis and design of microstrip interdigitated couplers," in *Proc. 6th European Microwave Conf.*, Rome, Sept. 1976, pp. 642–646.

[2] D. Pavlidis and H. L. Hartnagel, "The design and performance of three-line microstrip couplers," *IEEE Trans. Microwave Theory Tech.*, vol. MTT-24, pp. 631–640, Oct. 1976.

[3] S. Yamamoto *et al.*, "Coupled strip transmission line with three center conductors," *IEEE Trans. Microwave Theory Tech.*, vol. MTT-14, pp. 446–461, Oct. 1966.

[4] L. Bálint, "Modeling of coupled multiconductor microstrip-like transmission lines," *Int. J. Circuit Theory Appl.*, vol. 1, pp. 281–291, 1973.

[5] D. K. Marx, "Propagation modes, equivalent circuits and characteristic terminations for multiconductor transmission lines with inhomogeneous dielectrics," *IEEE Trans. Microwave Theory Tech.*, vol. MTT-21, pp. 450–457, July 1973.

[6] V. K. Tripathi, "Asymmetric coupled transmission lines in an inhomogeneous medium," *IEEE Trans. Microwave Theory Tech.*, vol. MTT-23, pp. 734–739, Sept. 1975.

Intermodulation Distortion Analysis of Reflection-Type IMPATT Amplifiers Using Volterra Series Representation

ALAUDDIN JAVED, BARRY A. SYRETT, MEMBER, IEEE, AND PAUL A. GOUD, SENIOR MEMBER, IEEE

Abstract—**Intermodulation distortion generated in a stable IMPATT amplifier is analyzed using Volterra series representation. An IMPATT amplifier model, which takes into account the interaction between the nonlinearities of the diode and its embedding circuitry, is described. The Volterra transfer functions are derived for this model. Nonlinear terms up to and including the fifth order are considered. Intermodulation distortion products are calculated for a low-level input signal consisting of two tones. The results of this analysis are extrapolated into the direction of increasing output power in order to obtain the third-order intercept point. Further, closed form expressions for the third-order intermodulation IM_3 and intercept point P_I are derived. The distortion of a specific 6-GHz IMPATT amplifier is evaluated for illustrative purposes; the predicted distortion behavior compares favorably with experimental results.**

Manuscript received May 18, 1976; revised March 7, 1977. The research reported in this paper was supported in part by the National Research Council of Canada under Grant NRC A-3725.

A. Javed is with Bell Northern Research, Ottawa, Ont., Canada K1Y 4H7.

B. A. Syrett is with the Applied Instrumentation Laboratory, Department of Electronics, Carleton University, Ottawa, Ont., Canada K1S 5B6.

P. A. Goud is with the Department of Electrical Engineering, University of Alberta, Edmonton, Alberta, Canada.

I. Introduction

MICROWAVE oscillators and amplifiers using IMPATT diodes are being utilized in areas such as telecommunications [1]. In many such applications, the intermodulation noise arising from IMPATT diode nonlinearities becomes an important consideration. This paper investigates the nonlinear distortion produced in an IMPATT amplifier, using Volterra series as an analysis tool. The Volterra series expansion allows a detailed and accurate

representation of device characteristics including memory effects. This technique has the additional advantage that closed form expressions of the third-order intermodulation distortion can also be obtained. Moreover, this approach can readily be extended to investigate the nonlinear behavior of other types of amplifiers [2]. This technique has been used by others for related studies of intermodulation distortion in video transistor amplifiers and in semiconductor diodes, for CATV applications [3]–[6].

In the present work, Volterra transfer functions are derived for an IMPATT diode amplifier model which takes into account the interaction of nonlinearities of the diode with the embedding circuitry. An appropriate expression representing the diode conductance and capacitance is used. At power levels where the diode nonlinearities are small, nonlinear terms up to and including the fifth order suffice to accurately characterize the nonlinear behavior of IMPATT amplifiers. The intermodulation distortion resulting from an applied two-tone signal is considered here. Komizo *et al.* [7] have described theoretical calculations of intermodulation products for a two-tone input, under the more restrictive assumptions that zero delay exists between a variation of the input signal level and the resulting RF voltage amplitude across the active device. The results obtained here at low signal levels can be extrapolated to the high signal level region, to obtain the intercept point P_I, between the fundamental and the third-order intermodulation products. For third-order nonlinearities, the intercept point P_I provides a convenient measure of the intermodulation performance of the device [8].

II. IMPATT Amplifier Model

Let us consider a simplified equivalent circuit for a circulator-coupled IMPATT amplifier, as shown in Fig. 1. It consists of a circulator, an impedance transformer, lumped-constant circuit elements, and an IMPATT diode. Although IMPATT amplifiers may be represented by more complex equivalent circuits, the simplified form shown in Fig. 1 can be used over a limited frequency range of specific interest [9]. An IMPATT diode may be represented at a constant operating current by a parallel combination of negative conductance $-G_n$ and capacitance C_j, since the imaginary component of the diode is capacitive at a normal frequency of operation. These diode parameters are nonlinear functions of the amplitude of the sinusoidal voltage V_d across the diode terminals and the frequency of this applied voltage. In IMPATT amplifiers having much less than octave bandwidth, as considered here, the variation of $-G_n$ and C_j over the amplifier passband is small and can be neglected. Further, the effect of odd-order terms in the power series expansion of $-G_n(V_d)$ and $C_j(V_d)$ on the fundamental current response is secondary to the effect of the even-order terms [8], [10]. Hence, over the amplifier passband, the nonlinear characteristics of the IMPATT diode may be expressed by

$$-G_n(V_d) = -g_n + \gamma V_d^2 + \sum_{n=2}^{\infty} a_n V_d^{2n} \tag{1}$$

$$C_j(V_d) = c_0 + \lambda V_d^2 + \sum_{n=2}^{\infty} b_n V_d^{2n} \tag{2}$$

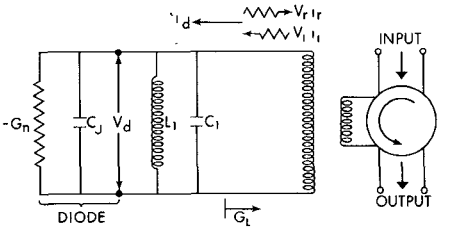

Fig. 1. Equivalent circuit used for distortion analysis of a reflection-type IMPATT amplifier.

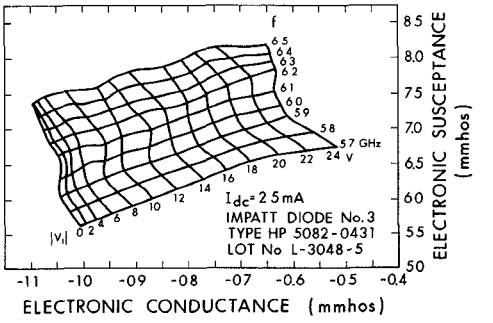

Fig. 2. Measured large-signal electronic admittance as a function of RF voltage amplitude and frequency.

where $-g_n$ and c_0 are small-signal values of the diode negative conductance and capacitance, respectively, under the given operating conditions; γ, λ, a_n, and b_n are constants. In the region of IMPATT amplifier operation considered here, where V_d is much smaller than the dc bias voltage, the terms for $n \geq 2$, in (1) and (2) may be neglected [9]. The constants γ and λ may be evaluated from the experimentally measured admittance plot of the particular IMPATT diode used. A typical diode admittance plot with diode RF voltage and frequency as parameters is shown in Fig. 2. The constants γ and λ for this diode are evaluated at the center of the frequency range to which the amplifier is tuned, and these values are found to remain almost constant throughout the limited frequency range of interest. The equivalent load admittance Y_L as seen from the diode terminals is

$$Y_L = G_L - j(1/\omega L_1 - \omega C_1). \tag{3}$$

The equivalent voltage and current components of the incident and reflected waves are represented by V_i, i_i, V_r, and i_r, where the subscripts i and r refer to incident and reflected waves, respectively. A circulator is used so that the input and output will appear at separate ports. The voltage across the diode terminals V_d and the net current i_d into the diode and parallel L_1C_1 network are given by

$$V_d = V_i + V_r \tag{4}$$

$$i_d = i_i - i_r = G_L(2V_i - V_d). \tag{5}$$

In the equivalent circuit of Fig. 1, i_d and V_d are governed by the following nonlinear integro-differential equation

$$i_d = C_1 \frac{dV_d}{dt} + \int_{-\infty}^{t} \frac{1}{L_1} V_d \, dt + \frac{d}{dt}(C_j V_d) - G_n V_d. \tag{6}$$

Substituting (1) through (5) [after ignoring the higher order terms $n \geq 2$ in (1) and (2)] into (6) and differentiating, we

obtain

$$2G_L\frac{dV_i}{dt} = (c_0 + C_1 + 3\lambda V_d^2)\frac{d^2V_d}{dt^2} + [G_L - g_n + 3\gamma V_d^2]\frac{dV_d}{dt} + 6\lambda V_d\left(\frac{dV_d}{dt}\right)^2 + L_1^{-1}V_d. \quad (7)$$

Equation (7) is a differential equation which specifies the nonlinear system under consideration within the constraints of our model.

III. Derivation of the Volterra Transfer Functions

A sufficient condition for the existence of Volterra series for a nonlinear system is that the operation of the system be restricted to a region of asymptotic stability [11]. This includes the stable IMPATT amplifiers under discussion. Thus it is assumed that the nonlinear system under consideration, specified by (7), can be represented by a Volterra series. We now proceed to calculate the Volterra transfer functions from the known system equations. For this purpose, we make use of the harmonic input method [12]. The harmonic input method is useful in computing $H_n(j\omega_1, j\omega_2, \cdots, j\omega_n)$ for the first few values of n. This method relies on the fact that a harmonic input must result in a harmonic output when a nonlinear system can be represented by a Volterra series. Thus when

$$V_i(t) = \exp(j\omega_1 t) + \exp(j\omega_2 t) + \cdots + \exp(j\omega_n t) \quad (8)$$

where $\omega_i = 2\pi f_i$, $i = 1, 2, \cdots, n$, and ω_i are incommensurable, H_n is given by

$$H_n(j\omega_1, j\omega_2, \cdots, j\omega_n) = \{\text{coefficient of the exp } [j(\omega_1 + \omega_2 + \cdots + \omega_n)]t \text{ term in the expansion of } V_d(t) \text{ in terms of } V_i\}. \quad (9)$$

Using (8) and (9) in (7), we obtain the first few Volterra transfer functions for the IMPATT amplifier model under consideration

$$H_1(j\omega_1) = \frac{j2\omega_1 G_L}{L_1^{-1} - (c_0 + C_1)\omega_1^2 + j\omega_1(G_L - g_n)} \quad (10)$$

$$H_2(j\omega_1, j\omega_2) = 0 \quad (11)$$

$$H_3(j\omega_1, j\omega_2, j\omega_3) = \frac{2(\omega_1 + \omega_2 + \omega_3)[j3\gamma - 3\lambda(\omega_1 + \omega_2 + \omega_3)]\prod_{i=1}^{3} H_1(j\omega_i)}{(c_0 + C_1)(\omega_1 + \omega_2 + \omega_3)^2 - L_1^{-1} - j(\omega_1 + \omega_2 + \omega_3)(G_L - g_n)} \quad (12)$$

$$H_4(j\omega_1, j\omega_2, j\omega_3, j\omega_4) = 0 \quad (13)$$

$$\begin{aligned} H_5(j\omega_1, j\omega_2, j\omega_3, j\omega_4, j\omega_5) &= [-6\lambda[\Sigma'_5\omega_1^2 H_1(j\omega_1) \cdot \{\Sigma'_4 H_1(j\omega_2)H_3(j\omega_3, j\omega_4, j\omega_5)\} \\ &+ \Sigma'_{10}H_1(j\omega_1)H_1(j\omega_2)H_3 \cdot (j\omega_3, j\omega_4, j\omega_5)(\omega_3 + \omega_4 + \omega_5)^2] \\ &+ j6\gamma[\Sigma'_5\omega_1 H_1(j\omega_1) \cdot \{\Sigma'_4 H_1(j\omega_2)H_3(j\omega_3, j\omega_4, j\omega_5)\} \\ &+ \Sigma'_{10}H_1(j\omega_1)H_1(j\omega_2)H_3 \cdot (j\omega_3, j\omega_4, j\omega_5)(\omega_3 + \omega_4 + \omega_5)] \\ &- 12\lambda[\Sigma'_5\omega_1 H_1(j\omega_1) \cdot \{\Sigma'_4(\omega_3 + \omega_4 + \omega_5)H_1(j\omega_2)H_3(j\omega_3, j\omega_4, j\omega_5)\} \\ &+ \Sigma'_{10}\omega_1\omega_2 H_1(j\omega_1)H_1(j\omega_2)H_3(j\omega_3, j\omega_4, j\omega_5)]]. \\ &[(c_0 + C_1)(\omega_1 + \omega_2 + \omega_3 + \omega_4 + \omega_5)^2 - L_1^{-1} \\ &- j(G_L - g_n)(\omega_1 + \omega_2 + \omega_3 + \omega_4 + \omega_5)]^{-1}. \end{aligned} \quad (14)$$

The even-order Volterra transfer functions are identically zero because the odd voltage terms in (1) and (2) can be neglected for narrow-band amplifier operation. In amplifiers with less than octave bandwidth nonzero even-order Volterra transfer functions would produce IM (intermodulation) distortion products which fall outside the passband.

IV. Computation of Intermodulation Distortion

For the measured equivalent circuit parameters and an input signal of the form

$$V_i(t) = V\cos\omega_1 t + V\cos\omega_2 t \quad (15)$$

the inband intermodulation products at $2\omega_1 - \omega_2$, $2\omega_2 - \omega_1$, $3\omega_1 - 2\omega_2$, $3\omega_2 - 2\omega_1$, etc., can be found.

One type of third-order intermodulation IM_3 can be defined as the ratio of the amplitude of the $(2\omega_1 - \omega_2)$ distortion product to the fundamental signal amplitude, in the output signal V_r. For the Volterra model, where nonlinear terms up to and including the fifth order are considered, the expression for IM_3 is

$$\text{IM}_3\ (\text{dB}) = 20\log\frac{V^2}{4|H_1(j\omega_1) - 1|}\,|3H_3(j\omega_1, -j\omega_2, j\omega_1) + 5V^2H_5(j\omega_1, -j\omega_1, j\omega_1, j\omega_1, -j\omega_2) + \tfrac{15}{2}V^2H_5(j\omega_1, j\omega_1, -j\omega_2, j\omega_2, -j\omega_2)|. \quad (16)$$

The last two terms in (16) represent the contribution from the fifth-order nonlinearity. The constants associated with the third- and fifth-order contribution in (16) are readily obtained by computing the steady-state response of the third- and fifth-order terms at the frequency $(2\omega_1 - \omega_2)$ for the input signal (15).

Similarly, one type of fifth-order intermodulation distortion IM_5 can be defined as the ratio of the amplitude of the $(3\omega_1 - 2\omega_2)$ distortion product to the fundamental signal amplitude in the output signal V_r. Since terms of higher

order than the fifth are not considered in the Volterra model, the expression for IM_5 is

$$IM_5\ (\text{dB}) = 20 \log \frac{5V^4 |H_5(j\omega_1, j\omega_1, j\omega_1, -j\omega_2, -j\omega_2)|}{8|H_1(j\omega_1) - 1|}. \tag{17}$$

For small distortion, an expression for IM_3 in terms of the parameters of the IMPATT amplifier model can be derived. In this case, the third-order term in the Volterra series is the major contribution to IM_3 and the H_5 term can be ignored. If we assume that 1) $\omega_1 \simeq \omega_2$, and 2) the carrier frequencies are very close to the resonant frequency, i.e., $\omega_1 \simeq \omega_2 \simeq \omega_0$, then

$$\omega_1 \simeq \omega_2 \simeq \omega_0 = [L_1(c_0 + C_1)]^{-1/2}. \tag{18}$$

Substituting (10) and (12) into (16), ignoring the H_5 term, and using the values of ω_1 and ω_2 given by (18), we obtain

$$IM_3\ (\text{dB}) \simeq 20 \log \frac{36[\gamma^2 + (\lambda\omega_0)^2]^{1/2}}{(G_L - g_n)^3(G_L + g_n)} G_L^3 V^2. \tag{19}$$

Using $V = (2P_{\text{in}}/G_L)^{1/2}$, we get

$$IM_3\ (\text{dB}) \simeq 20 \log \left\{ [\gamma^2 + (\lambda\omega_0)^2]^{1/2} \cdot \frac{G_L^2 P_{\text{in}}}{(G_L - g_n)^3(G_L + g_n)} \right\} + 37.2 \tag{20}$$

where P_{in} is the input signal power per tone.

Furthermore, in a two-tone test, the results obtained at low power levels can be extrapolated into the direction of increasing output power in order to define the third-order intercept point P_I (dBm) between the third-order distortion product and fundamental output power levels. For third-order nonlinearities, P_I is a convenient parameter for comparing the intermodulation performance of devices [8], [13]. From (10), (12), and (20), it can be shown that

$$P_I\ (\text{dBm}) = 10 \log \left\{ \frac{|(G_L + g_n)^3(G_L - g_n)|}{[\gamma^2 + (\lambda\omega_0)^2]^{1/2} G_L^2} \right\} + 11.43. \tag{21}$$

V. Comparison of Computed Distortion with Experimental Results

In this section, we apply the theory developed in the preceding sections to compute the intermodulation distortion products and intercept point for an IMPATT amplifier having the small-signal gain characteristics shown in Fig. 3. The experimental IMPATT amplifier was tuned for 17.3-dB gain at the center frequency 5.905 GHz, with a 3-dB bandwidth of 64 MHz. The electronic admittance of the experimental IMPATT diode has been measured as a function of RF voltage amplitude and frequency; the measured admittance is shown in Fig. 2. The small-signal parameters $-g_n$ and c_0, together with the nonlinearity constants γ and λ, were obtained by curve fitting (1) and (2) to these experimental results. Then the passive circuit parameters G_L, L_1, and C_1 of the equivalent circuit of Fig. 1 were chosen so that the amplifier model had approximately the same behavior over its passband as the measured gain response (see Fig. 3). The

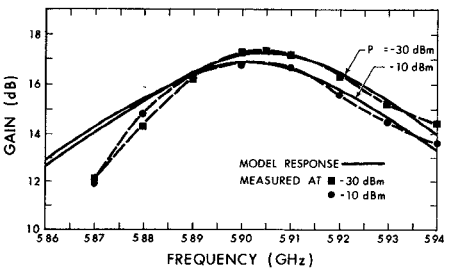

Fig. 3. Comparison of measured IMPATT amplifier gain with the gain predicted using the amplifier equivalent circuit ($I_{dc} = 25$ mA).

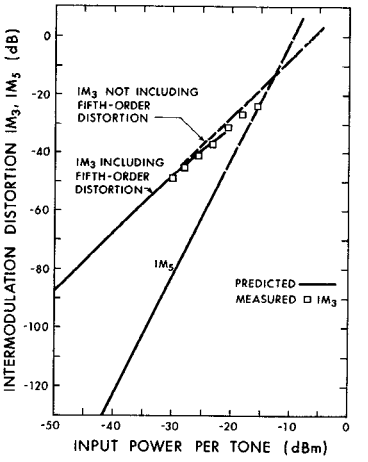

Fig. 4. Comparison of measured and predicted IM distortion for the experimental IMPATT amplifier ($I_{dc} = 25$ mA) with a two-tone input ($f_1 = 5.9045$ GHz, $f_2 = 5.9055$ GHz) at the center frequency.

values of the linear and nonlinear parameters of the model for the experimental IMPATT amplifier are listed in Table I.

Fig. 4 displays the calculated values of third- and fifth-order intermodulation distortion IM_3 and IM_5 for the experimental IMPATT amplifier at the center frequency 5.905 GHz. The two-tone input consisted of equal-level signals at 5.9045 and 5.9055 GHz (1 MHz apart). It is seen that, in the operating region resulting in small distortion considered here, the contribution of the fifth- and higher degree terms to IM_3 is small. Moreover, we observe that the magnitude of IM_5 is 60 dB below IM_3 at an input power level of -40 dBm, while at -20 dBm input IM_5 is only 19 dB below IM_3.

Intermodulation distortion was measured on a spectrum analyzer using a microwave two-tone generator for the input signal. This signal source employed the principle of a frequency-locked loop to produce a very stable 1-MHz frequency difference between two independent signal generators: 1) a klystron signal generator (HP 618C); 2) a varactor-tuned Gunn-effect oscillator (Varian VSC 9019S4). The 1-MHz reference signal was provided by a quartz crystal oscillator (HP 105A). The measured IM distortion is also plotted in Fig. 4. Measured third-order distortion IM_3 agrees with the predicted values within the expected measurement error of 1 dB. The fifth-order distortion IM_5 could not be resolved on the spectrum analyzer at input power levels below -20 dBm per tone.

Fig. 5 shows the behavior of IM_3 as a function of

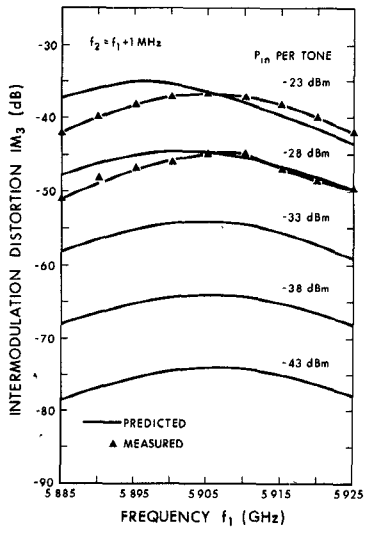

Fig. 5. Comparison of measured and predicted frequency dependence of third-order IM distortion for the experimental IMPATT amplifier ($I_{dc} = 25$ mA) with a two-tone input ($f_2 = f_1 + 1$ MHz).

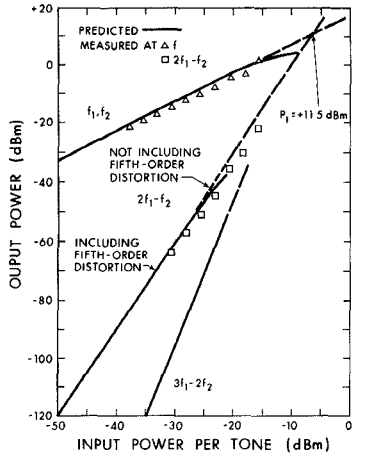

Fig. 6. Comparison of measured and predicted fundamental output and IM distortion products for the experimental IMPATT amplifier ($I_{dc} = 25$ mA) with a two-tone input ($f_1 = 5.9045$ GHz, $f_2 = 5.9055$ GHz) at the center frequency.

frequency in a 40-MHz frequency band around the amplifier center frequency. At small signal levels, the IM distortion is maximum at the center frequency, where the diode nonlinearities are coupled most strongly to the external passive circuit. For input signal levels near -23 dBm per tone, the amplifier gain begins to decrease, and the center frequency shifts to a lower frequency, as shown in Fig. 3. The predicted IM_3 also peaks at a lower frequency at this power level because of the shift in center frequency. The measured third-order distortion compares favorably with the predicted distortion: the discrepancy was less than 4 dB across the 40-MHz bandwidth.

The power in the fundamental component of the output signal, and the distortion power in the output signal are plotted as a function of input power in Fig. 6, for a two-tone input at the center frequency. The measured results are in good agreement with the predicted values. It can be seen that

TABLE I
IMPATT-AMPLIFIER NONLINEAR MODEL PARAMETERS

PARAMETER	VALUE	DIMENSION
$-g_n$	-1.027	mS
c_0	0.1643	pF
c_1	0.6430	pF
L_1	0.8998	nH
G_L	1.351	mS
γ	8.651×10^{-4}	mS/V^2
λ	6.288×10^{-5}	pF/V^2

at 0 dBm total output power, the total third-order distortion is -35 dBm, and the total fifth-order distortion is -48 dBm. The results at low power levels have been extrapolated into the high power region, to obtain the third-order intercept P_I for the experimental IMPATT amplifier. The experimental P_I, 12 dBm, is in good agreement with the predicted value 11.5 dBm; $P_I = 11.3$ dBm is calculated from (21) using the values in Table I. To put this result into perspective, a P_I of 29 dBm was reported recently for a highly linear, 11-GHz FET amplifier operating at an output power level of 19.5 dBm [13].

VI. CONCLUSION

This paper has presented a useful technique for analyzing the intermodulation distortion produced in a stable IMPATT amplifier. This technique allows the derivation of closed form expressions for the third-order intermodulation IM_3, and intercept point P_I, from experimentally measured single tone parameters. The results obtained from this technique compare favorably with experimental results.

REFERENCES

[1] H. Komizo *et al.*, "A 0.5-W CW IMPATT diode amplifier for high capacity 11 GHz FM radio-relay equipment," *IEEE J. Solid-State Circuits (Special Issue on Microwave Integrated Circuits)*, vol. SC-8, pp. 14–20, Feb. 1973.

[2] A. Javed, P. A. Goud, and B. A. Syrett, "Analysis of a microwave feed-forward amplifier using Volterra series representation," *IEEE Trans. Commun.*, vol. COM-25, pp. 355–360, Mar. 1977.

[3] S. Narayanan, "Transistor distortion analysis using Volterra series representation," *Bell Syst. Tech. J.*, pp. 991–1024, May–June 1967.

[4] — —, "Intermodulation distortion of cascaded transistors," *IEEE J. Solid-State Circuits*, vol. SC-4, pp. 97–106, June 1969.

[5] R. E. Maurer and S. Narayanan, "Intermodulation distortion analysis of transistor nonlinearities with a random input," *IEEE Trans. Commun. Tech.*, vol. COM-16, pp. 701–712, Oct. 1968.

[6] A. Prochazka and R. Neuman, "High-frequency distortion analysis of a semiconductor diode for CATV applications," *IEEE Trans. Consumer Electronics*, vol. CE-21, pp. 120–129, May 1975.

[7] H. Komizo *et al.*, "Improvement of nonlinear distortion in an IMPATT stable amplifier," *IEEE Trans. Microwave Theory Tech.*, vol. MTT-21, pp. 721–728, Nov. 1973.
[8] G. L. Heiter, "Characterization of nonlinearities in microwave devices and systems," *IEEE Trans. Microwave Theory Tech.*, vol. MTT-21, pp. 797–805, Dec. 1973.
[9] H. J. Kuno, "Analysis of nonlinear characteristics and transient response of IMPATT amplifiers," *IEEE Trans. Microwave Theory Tech.*, vol. MTT-21, Nov. 1973.
[10] M. E. Hines, "Negative-resistance diode power amplification," *IEEE Trans. Electron. Devices*, vol. ED-17, pp. 1–8, Jan. 1970.
[11] H. Van Trees, *Synthesis of Optimum Nonlinear Control Systems.* Cambridge, MA: M.I.T. Press, 1962.
[12] E. Bedrosian and S. O. Rice, "The output properties of Volterra systems (nonlinear systems with memory) driven by harmonic and Gaussian inputs," *Proc. IEEE*, vol. 59, pp. 1688–1707, Dec. 1971.
[13] P. Bura *et al.*, "Highly linear medium power, 11 GHz FET amplifier," *ISSCC Digest of Technical Papers*, pp. 158–159, Feb. 1976.

Effects of Depletion-Layer Modulation on Spurious Oscillations in IMPATT Diodes

D. TANG, MEMBER, IEEE, AND G. I. HADDAD, FELLOW, IEEE

Abstract—**A theoretical analysis of the effects of depletion-layer modulation on spurious oscillations in IMPATT diodes is given. The relationship between the magnitude of the depletion-layer modulation, circuit impedance and threshold for degenerate instabilities is presented.**

I. Introduction

IMPATT diode microwave amplifiers and oscillators frequently exhibit certain spurious "parametric oscillations" near or at the subharmonic of the signal frequency, when the RF excitation exceeds a threshold level, which is dependent upon the device and circuit and often occurs below the power saturation point. Hines [1], Peterson [2], and Schroeder [3] gave detailed analyses on these parametric effects for a Read-type diode. They analyzed the parametric instabilities based on the nonlinear relationship between the avalanche current and the voltage across the avalanche region. Parametric components (at frequencies other than the pump frequency but whose sum is equal to the pump frequency) may exist in these devices. These current components flow through the drift region, experience a phase change and induce a current in the external circuit. The interaction between the current components and the circuit may lead to self-sustaining voltages at these parametrically related frequencies even without any external sources at these frequencies. The expressions for determining the instability threshold were given in [1, eqs. (23) and (35)]. It was emphasized there that circuit impedance may either suppress or enhance the occurrence of the instability. Based on the work of Hines [1], Schroeder [3] derived the circuit impedance conditions required for unconditional stable operation and for avoiding parametric instabilities in the IMPATT diode circuit.

Generally, the IMPATT diode has a nonpunch-through structure and its depletion-layer width is modulated considerably by the RF voltage [4], [5]. The objective of the present investigation is to examine the effect of the depletion-layer-width modulation on the parametric instabilities. The original analysis of [1] concerning the parametric components in the avalanche region is retained [1, (1)–(16)]. The change of the phase relationship in the drift region is examined including the nonlinear capacitance effect, and due to the complexity of the mathematics some assumptions are made. These assumptions and results are discussed as they arise.

II. Theoretical Analysis

A typical high-efficiency structure for an IMPATT diode is selected for this analysis. It is of the low–high–medium doping type. Fig. 1 shows the electric field profile of this structure. The metallurgical junction is at $x = 0$. The diode is divided conceptually into an avalanche region with fixed width x_a and a drift region with a time-varying width x_d, which is approximately proportional to the square root of the terminal instantaneous voltage. The RF terminal voltage consists of two parts. One is the large microwave periodic excitation, called the pump signal, at frequency ω_p, and the other is a small applied signal at frequency ω_0, which may or may not be harmonically related to the pump frequency. This small signal is applied as a perturbation and is assumed to be sinusoidal. Because of the nonlinearity of the avalanche process, multiple responses occur at various new frequencies that are sums and differences of the various harmonics of the frequencies applied. The main interest here

Manuscript received September 15, 1975; revised November 15, 1976. This work was supported by the Air Force Systems Command, Rome Air Development Center, under Contract F30602-74-C-0012. It was also partially sponsored by the Air Force Office of Scientific Research, Air Force Systems Command, USAF, under Grant AFOSR-76-2939.

D. Tang is with IBM, Thomas J. Watson Research Center, Yorktown Heights, NY 10598.
G. I. Haddad is with the Department of Electrical and Computer Engineering, University of Michigan, Ann Arbor, MI 48109.